Seismic reservoir characterization of Utica-Point Pleasant shale with efforts at fracability evaluation — Part 2: A case study

Ritesh Kumar Sharma[1], Satinder Chopra[1], James Keay[2], Hossein Nemati[1], and Larry Lines[3]

Abstract

The Utica Formation in eastern Ohio possesses all the prerequisites for being a successful unconventional play. Attempts at seismic reservoir characterization of the Utica Formation have been discussed in part 1, in which, after providing the geologic background of the area of study, the preconditioning of prestack seismic data, well-log correlation, and building of robust low-frequency models for prestack simultaneous impedance inversion were explained. All these efforts were aimed at identification of sweet spots in the Utica Formation in terms of organic richness as well as brittleness. We elaborate on some aspects of that exercise, such as the challenges we faced in the determination of the total organic carbon (TOC) volume and computation of brittleness indices based on mineralogical and geomechanical considerations. The prediction of TOC in the Utica play using a methodology, in which limited seismic as well as well-log data are available, is demonstrated first. Thereafter, knowing the nonexistence of the universally accepted indicator of brittleness, mechanical along with mineralogical attempts to extract the brittleness information for the Utica play are discussed. Although an attempt is made to determine brittleness from mechanical rock-physics parameters (Young's modulus and Poisson's ratio) derived from seismic data, the available X-ray diffraction data and regional petrophysical modeling make it possible to determine the brittleness index based on mineralogical data and thereafter be derived from seismic data.

Introduction

Horizontal drilling and multistage fracturing have now made it possible to develop and exploit unconventional reservoirs that were once thought of principally as source rocks. With the successful development of unconventional shale reservoirs worldwide and especially across North America, the oil and gas industry has shifted its attention to a Utica Formation in Ohio because its organic richness, high content of calcite, and development of extensive organic porosity make it a potential unconventional play (Patchen and Carter, 2012). The Utica Formation is believed to be the source rock that holds more than 300 million barrels of oil and three trillion cubic feet of gas reserves from overlying Clinton sandstones and deeper Cambrian-Ordovician age Knox carbonates and sandstones in eastern Ohio.

The geologic setting of the study area and 3D seismic data acquisition and processing have been discussed by authors in an expanded abstract and part 1 of this paper (Chopra et al., 2017, 2018). In fact, the primary target zone in the Utica play includes the basal Utica, an organic calcareous shale, Point Pleasant, an organic-rich carbonate interbedded with calcareous shale that underlies Utica, and the upper Trenton of the Black River group, an organic-rich carbonate that underlies Point Pleasant. The three zones represent a transgressive system tract, in which the shallow shelf carbonates of the Trenton were cyclically flooded by rising seas. For the present study, the Point-Pleasant interval has been considered as the zone of interest. The interval in the target formation that exhibits high total organic carbon (TOC) content, high porosity, as well as high brittleness is believed to be the most favorable drilling zone. These conclusions are based on the facts that the higher the TOC and porosity in a formation, the better its potential for hydrocarbon generation, and the higher the brittleness, the better its fracability. Therefore, any approach of providing information about TOC, porosity, and brittleness using seismic data could be useful for the delineation of sweet spots in a lateral sense. Petrophysical modeling carried out in the target formation regionally using well-log data as well as core samples reveals a strong relationship of bulk density with TOC and porosity (Patchen and Carter, 2012). Thus, organic-rich and porous zones can be identified if somehow density is estimated from the seismic data. Such

[1]TGS, Calgary, Alberta, Canada. E-mail: rsharma@arcis.com; satinder.chopra@tgs.com; mnemati@arcis.com.
[2]TGS, Houston, Texas, USA. E-mail: james.keay@tgs.com.
[3]University of Calgary, Calgary, Alberta, Canada. E-mail: lrlines@ucalgary.ca.

First presented at the SEG 87th Annual International Meeting. Manuscript received by the Editor 31 July 2017; revised manuscript received 11 October 2017; published ahead of production 15 December 2017; published online 16 March 2018. This paper appears in *Interpretation*, Vol. 6, No. 2 (May 2018); p. T325–T336, 12 FIGS.
http://dx.doi.org/10.1190/INT-2017-0135.1.

pockets can then be transformed into sweet spots once brittleness information is available. Attempts have been made to identify the brittle zone based on the Young's modulus and Poisson's ratio. The computation of the former requires the availability of density. Consequently, the estimation of density from seismic data is required for mapping the sweet spots laterally in the Utica play.

Density estimation from seismic

There are usually two conventional ways of estimating density from seismic data. One way is to use vertical component seismic data that contain noise-free long-offset data. It can also be determined from the recorded multicomponent seismic data. However, the unavailability of either data set in the present area of study leads us to explore other alternative methods of computing density from available seismic data. Multiattribute regression analysis and a probabilistic neural network (PNN) approach could be alternative ways for the purpose. But, the accuracy of this approach may depend on how uniformly a sufficient number of wells are distributed on the 3D seismic data being used for reservoir characterization. Although a sufficient number of wells with a density curve were found to be distributed uniformly on the 3D seismic data at hand, sonic curves were missing for most of them. The absence of the sonic curve at different wells restrains us from using them in the neural network analysis, as the time-depth relationship is a prerequisite for executing any approach on the seismic data that are recorded in the time domain. In such a scenario, sonic curves can be predicted from available density curves using Gardner's equation or an equivalent equation calibrated locally. For doing so, a crossplot of measured density and velocity available for seven wells is generated as shown in Figure 1. The seven wells mentioned here are indicated in Figure 4 of part 1 of this paper (Chopra et al., 2018). A poor correlation (15%) between the attributes plotted suggests that an alternative method is required. Multiattribute analysis, in which multilinear transformation is used to predict a target log from the combinations of other logs, could have been followed if consistency had existed in terms of available measured well logs for all the considered wells. As gamma ray (GR) and density curves were consistent for all the wells, P-velocity was crossplotted with GR curves, as shown in Figure 2a. The cluster of points on the crossplot shows a correlation coefficient of 0.68, which is better than that obtained between P-velocity and density. However, although the linear relationship is indicated for a majority of points, for those points enclosed in the ellipse and which are coming from our zone of interest, the linear relationship would overestimate the P-velocity. In Figure 2c (track 1), we illustrate the overestimated sonic curve in blue compared with the measured curve in red in a well, in which the data were available in the zone of interest. Similarly, when synthetic seismograms are generated using overpredicted sonic curves and compared with the real seismic data, a mismatch is noted in the zone of interest (Figure 3a). Examination of the points enclosed in the ellipse, which are coming from our zone of interest in Figure 2a, suggests that these points exhibit low values of GR. This seems contradictory to what is generally observed, i.e., the high GR response being related with organic richness. Although this is the case here, an explanation for this observation is in order. Organic material in rocks is generally associated with high values of GR due to the absorption of uranium from seawater when they are deposited. This usually happens when the deposition takes place in a low-energy anoxic environment, so that there is enough time for the organic material to absorb the dissolved uranium in seawater. The uranium content is also reflected in spectral GR log curves as the uranium curve exhibits higher signatures corresponding to zones with high TOC.

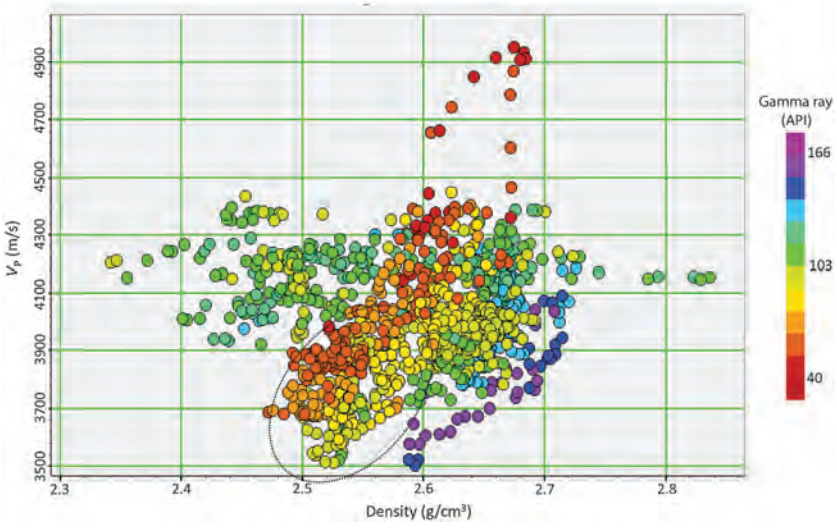

Figure 1. Crossplot of V_P versus density for available wells that have measured curves, color coded with GR. The large scatter of cluster points suggests that the method cannot be used to determine velocity from density logs. Points enclosed by an ellipse come from the zone of interest and exhibit low values of all the measured logs used in this crossplot.

In areas where organic material is present but the deposition took place in a high-energy environment, the organic material most likely did not get a chance to absorb the uranium, and in such cases, most likely the GR signature would be low. Similarly, the uranium spectral GR curve will also show lower values. In the case under investigation, the depositional environment of the Point-Pleasant Formation was a relatively shallow storm-dominated, carbonate shelf, which probably explains why the low GR signatures correlate with TOC.

Another interesting observation from the regional analysis over the Utica play is that the organic richness is correlated more with the carbonate content (Patchen and Carter, 2012) than the other minerals. As porosity and organic richness affect the sonic and density curves in a similar manner, a positive relationship must exist between them in our zone of interest. A second look at Figure 1, especially for points in the ellipse does indeed show a linear relationship between velocity and density. It should therefore be possible to correct the overprediction of sonic curves by considering the density curves.

Correction for over prediction of P-velocity

In our attempt to correct for the overprediction of P-velocity, especially in the zone of interest, we first compute delta V_P, the difference between the measured and predicted P-velocity values. Although the delta V_P is close to zero above and below the zone of interest as expected, it is positive over the zone of interest, as we see in track 3 of Figure 2c. We are already aware that the density would be low in the zone of interest due to its strong relationship with TOC observed in the Utica Formation (Wang et al., 2016). Thus, we crossplot the delta V_P values with density and derive the linear relationship, as shown in Figure 2b. This relationship was then used to predict delta V_P (in the zone of interest) from the available density curves, which are more readily available and consistent than the sonic curves. Having delta V_P, the overpredicted values of V_P are then corrected. The corrected and uncorrected curves are shown in track 4, and the corrected and the measure P-velocity curves are shown in track 5 of Figure 2c. It is observed that the two curves overlay each other. Thus,

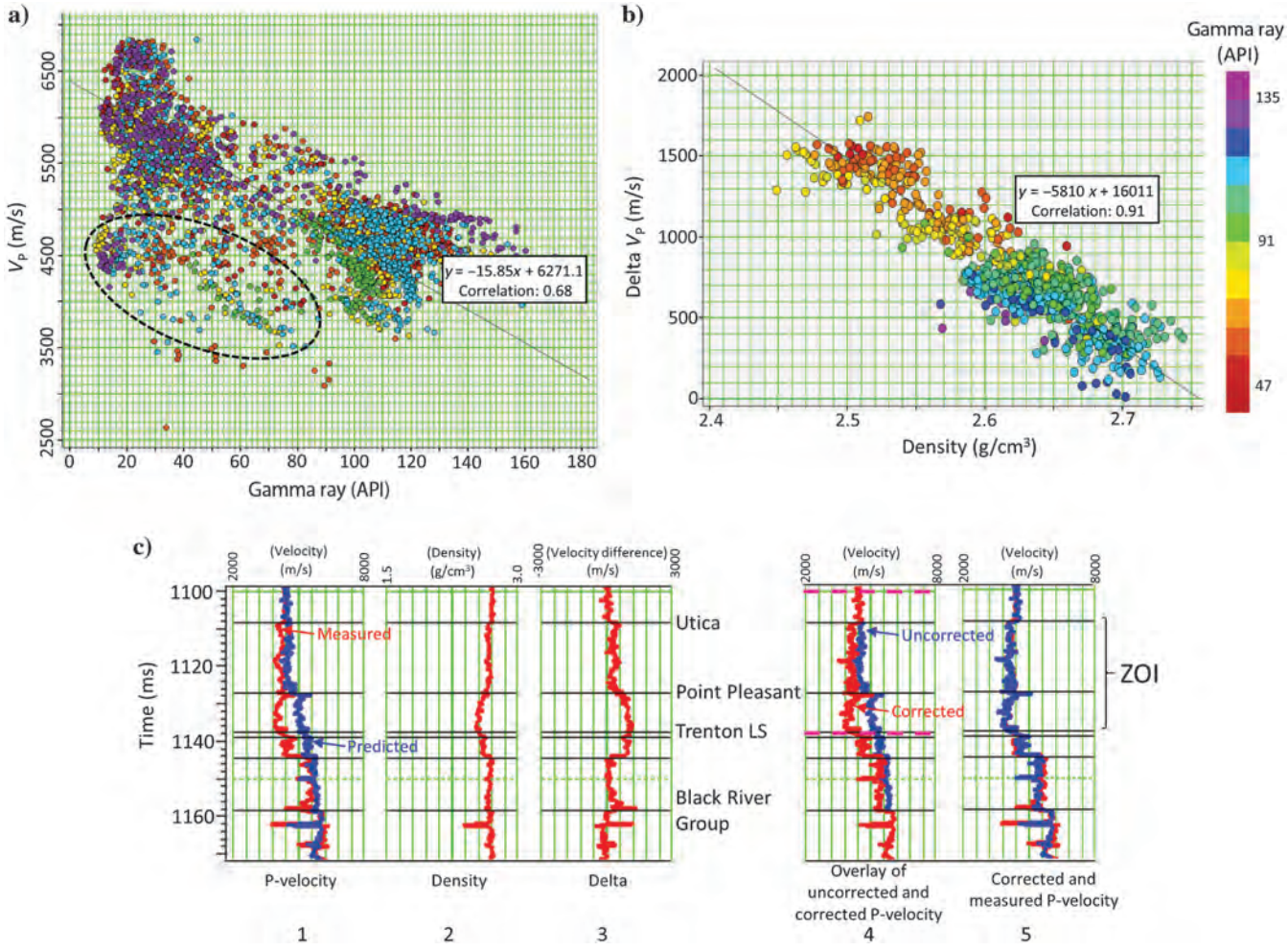

Figure 2. (a) Crossplot of P-velocity (V_P) versus GR for available wells that have measured curves, color-coded with the well name. A correlation of 68% is noticed. Using the above relationship, prediction of the P-wave velocity would be overestimated for the points enclosed by ellipses in black. (b) Crossplot of density versus delta V_P (the difference between predicted sonic and measured sonic) over the interval bounded by dashed pink bars shown in Figure 2c color coded with GR. A linear relationship exists between them, which can be used to correct the overestimation of the sonic curve that is made using the GR curve. (c) Track 1shows the over-predicted sonic curve overlaid with the measured curve. Track 2 show the density curve, and track 3 is the difference curve between the predicted sonic and measured sonic. Track 4 shows the overlay of the uncorrected and correct sonic curves, and track 5 shows the predicted and measure sonic curves. Notice the accurate match between the predicted and measured sonic curves, which enhances our confidence in using this approach.

when the overestimated sonic curve is predicted using the GR curve, a correction is made by considering the density-log curve. A similar observation is made for all the other wells.

Furthermore, not relying just on the visual examination, when the predicted and measured sonic-log curves are crosscorrelated, a large correlation coefficient is seen, which adds confidence in the predictions made by the workflow. This workflow is found useful in the present analysis because the GR and density curves are available in a large number of wells over the 3D volume and are also uniformly distributed. These are then used to predict reliable sonic-log curves, which in turn are used to obtain the depth-time relationships for well ties, in which a high correlation is observed (Figure 3b). With the availability of sonic and density curves at uniformly distributed wells over the 3D seismic volume, it is now possible to make use of multiattribute regression and neural network workflows for determination of density as discussed below.

Density prediction using neural network approach

The PNN implementations have been applied to a variety of geophysical problems (Hampson et al., 2001; Leiphart and Hart, 2001). In such an approach, a nonlinear relationship is determined between seismic data as well as its various attributes and petrophysical properties. The determined relationship is then used to predict the desired properties away from the well control. For the present study, a multiattribute linear regression and PNN are implemented to predict the density volume for estimating the TOC volume. We first derive the relevant attributes for our study by applying a prestack simultaneous inversion to conditioned gathers using partial-angle stacks, a reliable low-frequency model and angle-dependent wavelets. The details of individual processes are provided in the companion paper (Chopra et al., 2017, 2018). However, prestack simultaneous inversion analysis carried out at blind well location is shown in Figure 4 to show the reliability of the inverted attributes. The attributes derived from the simultaneous inversion are P-impedance, S-impedance, lambda-rho, mu-rho, E-rho, and Poisson's ratio volumes. A combination of these different attributes is input to the multiattribute regression and PNN process to predict density. An important aspect of this method is the selection of seismic attributes to be considered in the neural network training. To that effect, a multiattribute stepwise linear regression analysis (Hampson et al., 2001) is performed using available uniformly distributed wells. An optimal number of attributes and the operator length are selected using the crossvalidation

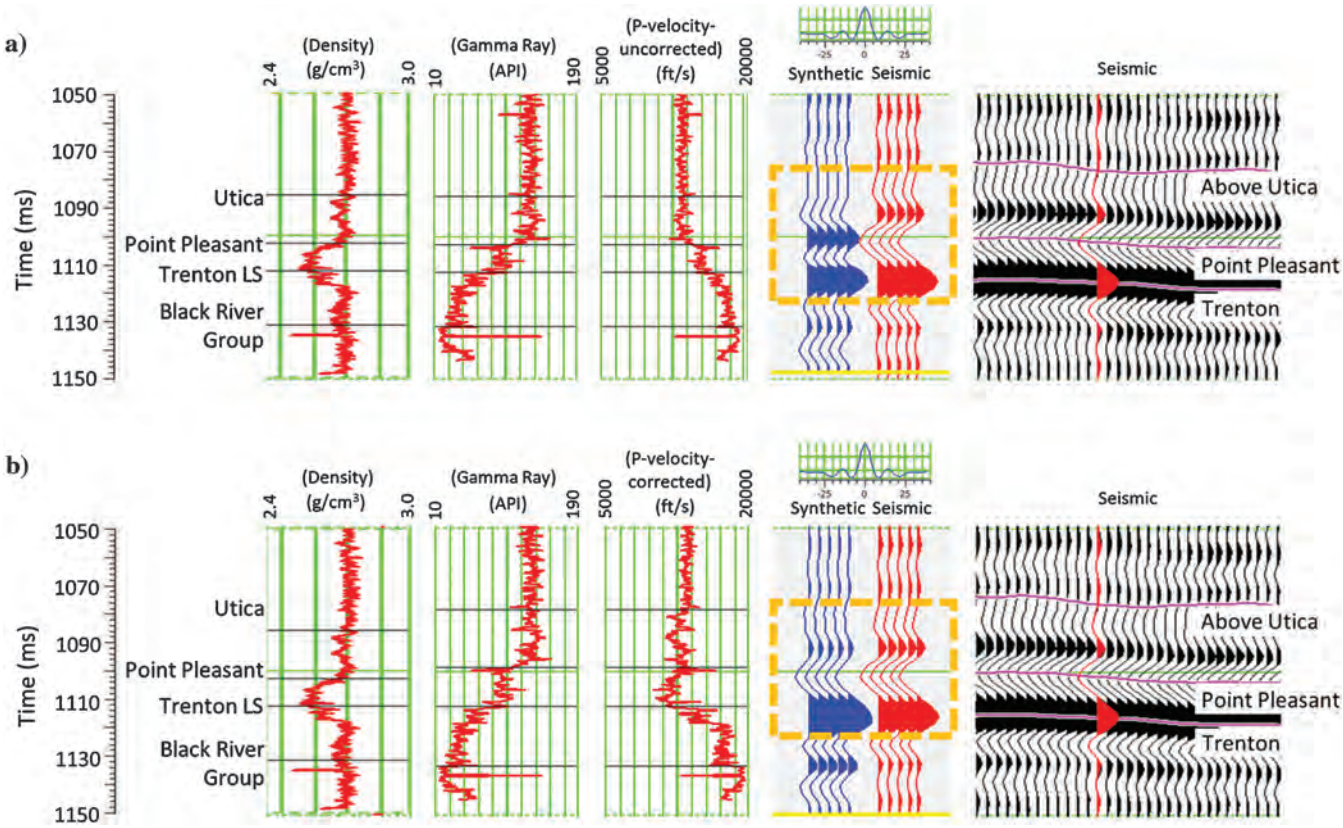

Figure 3. (a) Well-to-seismic tie for a well over the zone of interest, in which the sonic curve was missing and its prediction was made from GR using the determined relationship. A poor correlation between synthetic (blue traces) and real data (red traces) is noticed when over-predicted velocity is used to generate the synthetic data. (b) A similar tie is shown where the predicted log curve after correction was used for generating the synthetic.

criteria (Hampson et al., 2001), in which one well at a time is excluded from the training data set and the prediction error is calculated at the excluded well location. The analysis is repeated for all the wells, each time excluding a different well. An operator length of nine samples exhibited the minimum validation error with six attributes, as shown in Figure 5a. The attributes are Poisson's ratio, E-rho, relative impedance, absolute P-impedance, S-impedance, and a filtered version of the input seismic data. Using these attributes, the PNN was trained. A correlation of 98.12% is noted between predicted and measured densities at the well locations. After training, a validation process was followed, which showed a correlation of 93.59% (Figure 5b) at the well locations. A representative section from the predicted density volume along an arbitrary line that passes through different wells is shown in Figure 6. The measured density curve is inserted as a variable color log on this section. A very good match between the inserted curve and predicted density is seen. Such a match enhances the confidence in the analysis of predicting density. A variation of density values within the zone of interest is also noted as we go from the northern to the southern side of the 3D survey.

Density/TOC transformation

Kerogen or organic matter exhibits low density compared with the primary density range of minerals in mudrocks. Hence, density decreases as TOC content increases. A similar observation is found to exist in the Utica-Point Pleasant Formations. The density and TOC measurement made on the core samples in the zone of interest are crossplotted by Wang et al. (2016), as shown in Figure 7a. Five representative wells from the Appalachian Basin and close to the area of our interest are used to generate this crossplot. A strong linear relationship is seen between density and TOC as expected. Furthermore, this relationship is calibrated with the available core data for the present area of study. Figure 7b shows the match between predicted TOC and measured from the core samples for the area of study after proper calibration. A reasonable match between them endorses the relationship, which is then used to transform the predicted density volume into a TOC volume. To map the variation of TOC content laterally, a horizon slice from its volume over a 10 ms window in the zone of interest is generated as shown in Figure 7c; low-TOC zones are indicted by yellowish and bluish colors, whereas black and gray colors represent high-TOC zones. Note that higher TOC values are seen in the northern part of the survey than the southern zone, which is consistent with the prior information available regionally and matches the available production data (green circles). It may be mentioned here that the production data have been obtained from the online open database, and we are not sure about its accuracy. However, the match seems convincing.

Brittleness and fracability determination

A successful shale resource play can be identified based on such properties as the maturation, mineralogy, pore pressure, thickness, organic richness, permeability, brittleness, and gas in place (Chopra et al., 2012; Verma et al., 2016). Brittleness is a key property that reservoir engineers are interested in as brittle rocks fracture much better than ductile rocks and enhance the permeability. Thus, it is desirable for shale source rocks to exhibit high brittleness. The brittleness of a formation is associated with its mineral content (Jarvie et al., 2007). Initially, it was thought that the presence of quartz mineral in a formation makes it more brittle, whereas more clay makes it ductile. Later, it was observed that the presence of dolomite tends to increase the brittleness of a shale play (Wang and Gale, 2009). Further, Jin et al. (2015) note that instead of dolomite, the carbonate contribution (dolomite/calcite) should be considered for computation of brittleness. These authors proposed a brittleness index (BI) for identification of brittle zones in a shale play as follows:

$$\mathrm{BI}_{\mathrm{mineralogy}} = \frac{(W_{\mathrm{quartz}} + W_{\mathrm{calcite}} + W_{\mathrm{dolomite}})}{W_{\mathrm{total}}}, \qquad (1)$$

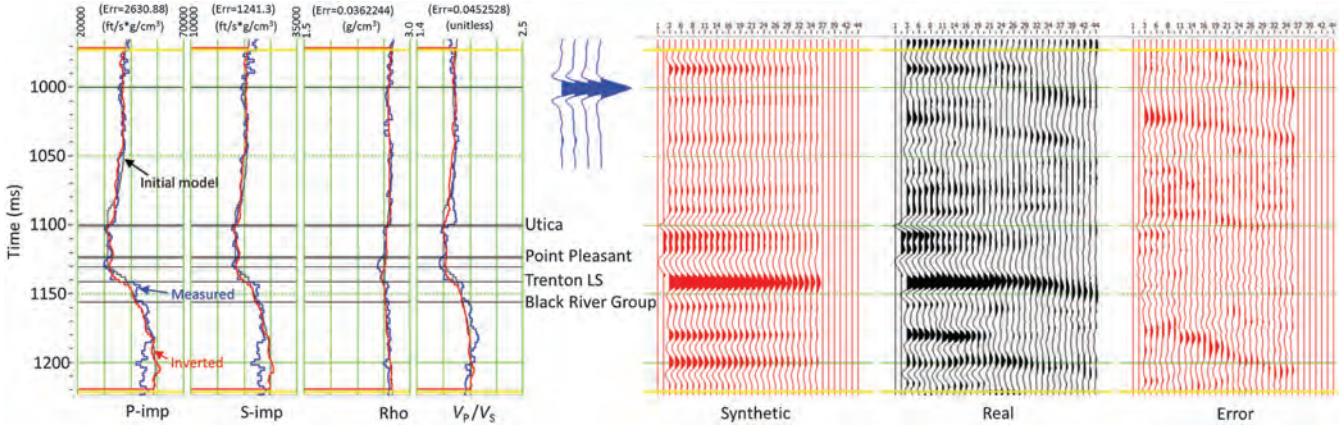

Figure 4. Prestack simultaneous inversion analysis carried out at blind well location. A reasonable match between inverted and measured attributes is noticed, which enhances our confidence in the inversion process.

where W corresponds to the weight fraction. Thus, an investigation of different minerals in the zone of interest leads to the identification of favorable drilling zones. Normally, it is an arduous task to compute the individual mineral content of a formation using seismic data, and geoscientists rely on the Young's modulus and Poisson's ratio attributes (Sharma and Chopra, 2015). However, for the present study, the available X-ray diffraction data show that quartz, calcite, and clay are the main minerals present in the Utica play. Additionally, regional petrophysical modeling carried out for the condensate region reveals a strong relationship of clay volume (V_{clay}) with the neutron porosity minus density porosity (NMD) data. Furthermore, the quartz group (quartz + feldspar) and the carbonates group (calcite + dolomite) showed a strong relationship with the neutron porosity curve (NPHI), as shown in Figure 8. Therefore, the volumes of neutron porosity and density porosity (DPHI) should be computed, so that the mineralogical content of the Utica play can be obtained. For doing so, first we cross plot the neutron porosity and density porosity with those attributes from well-log data that can be seismically derived. Thereafter, we select those attributes that show a good correlation, so that the relationship could then be used for transforming the seismically derived attributes into neutron porosity and density porosity. Such a crossplot of these two curves with the measure P-impedance and density over the Point Pleasant interval is shown in Figure 9.

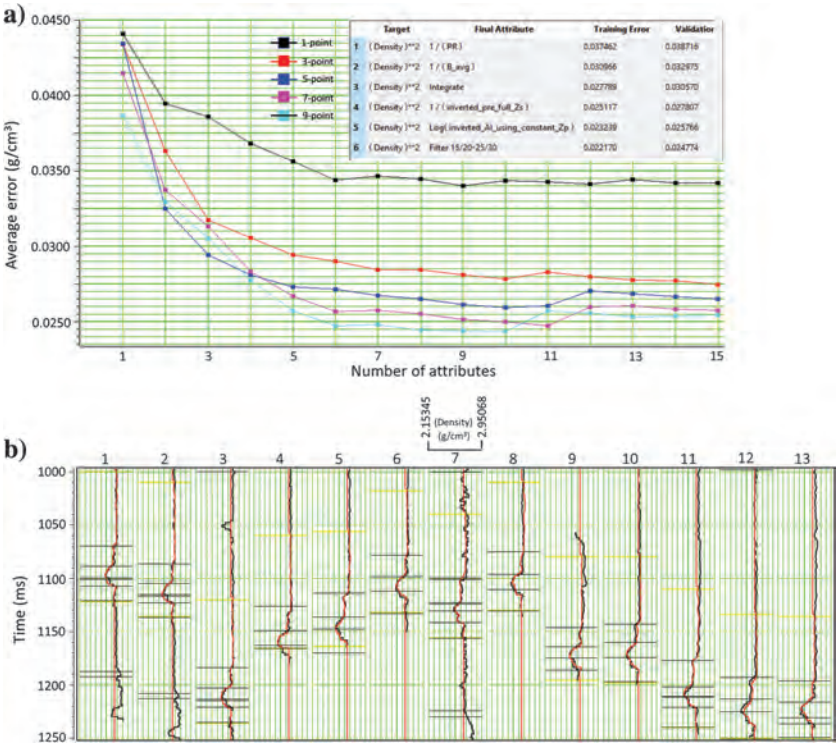

Figure 5. (a) Selection of optimal number of attributes and the operator length for neural network analysis. An operator length of nine samples with six attributes exhibited minimum validation error. After the training phase, a validation process was followed and the results are shown in (b). The display range for all the density curves is the same and is shown on the top. Notice a correlation of 93.59% between the predicted (red) and measured (black) density curves.

As there is good correlation between P-impedance and NPHI and density as well as DPHI, we can use these respective relationships for deriving NPHI and DPHI volumes from P-impedance and density volumes. A similar analysis is carried out for the Utica interval, and we notice a good correlation between DPHI and density but a better correlation for S-impedance and NPHI. These determined relationships are then used for deriving NPHI and DPHI volumes from inverted P- and S-impedance and density.

As mentioned before, simultaneous prestack impedance inversion was run on the data and P- and S-impedance attributes realized therefrom. Next, the determined relationships discussed above were used to transform the inverted attributes (P- and S-impedances and density) into individual mineral con-

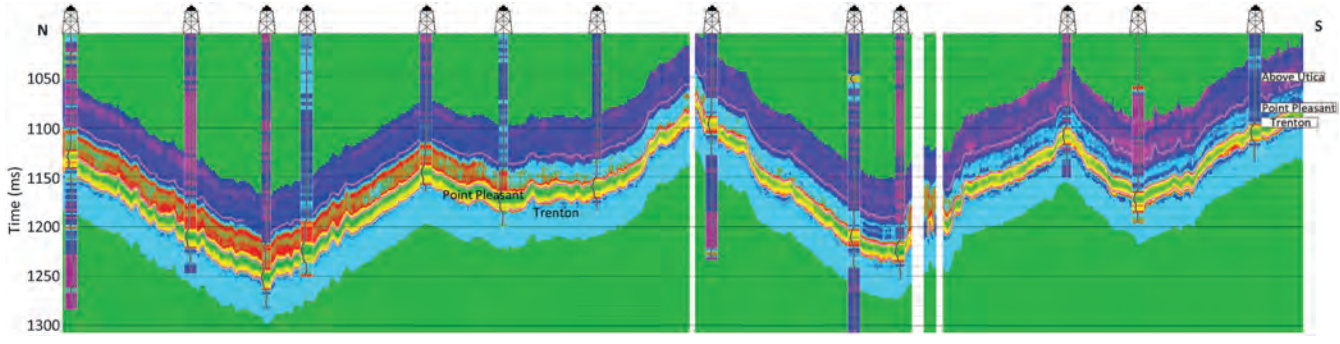

Figure 6. An arbitrary line passing through different wells in the density volume generated neural network approach. The measured density logs have been inserted as variable density color log. A variation of density can be seen vertically as we go from Utica interval to Trenton. Additionally, lateral variation of density can be noticed within the individual intervals.

tent volume. Their vertical sections along an arbitrary line that passes through different wells are shown in Figure 10. It was noticed here that more than 40% clay content exists in the Utica interval, and it decreases as we go from Utica to Trenton. Quartz group content varies from 20% to 40% for Utica and Point Pleasant intervals, being higher in the former than the latter. Additionally, carbonate content decreases as we go from Trenton to Utica interval. Thus, the Point Pleasant interval contains more carbonate content than the Utica interval and seems to be more brittle. We find this observation to be consistent with the petrophysical information available in the area of study, and it lend the confidence in the prediction of different mineral contents. With these individual mineral volumes now computed, the BI attribute was derived using equation 1. A horizon slice from this mineralogical BI volume over the Point Pleasant interval is shown in Figure 11a. Pockets with high values of brittleness are indicated in the light-blue, dark-blue, and magenta colors. The northern part on this display seems to be more brittle because it exhibits higher values of BI.

This observation correlates well with the hydrocarbon production data from the Point Pleasant interval, as indicated with the green circles. The data from the peak initial production rate (PIPR) were also available

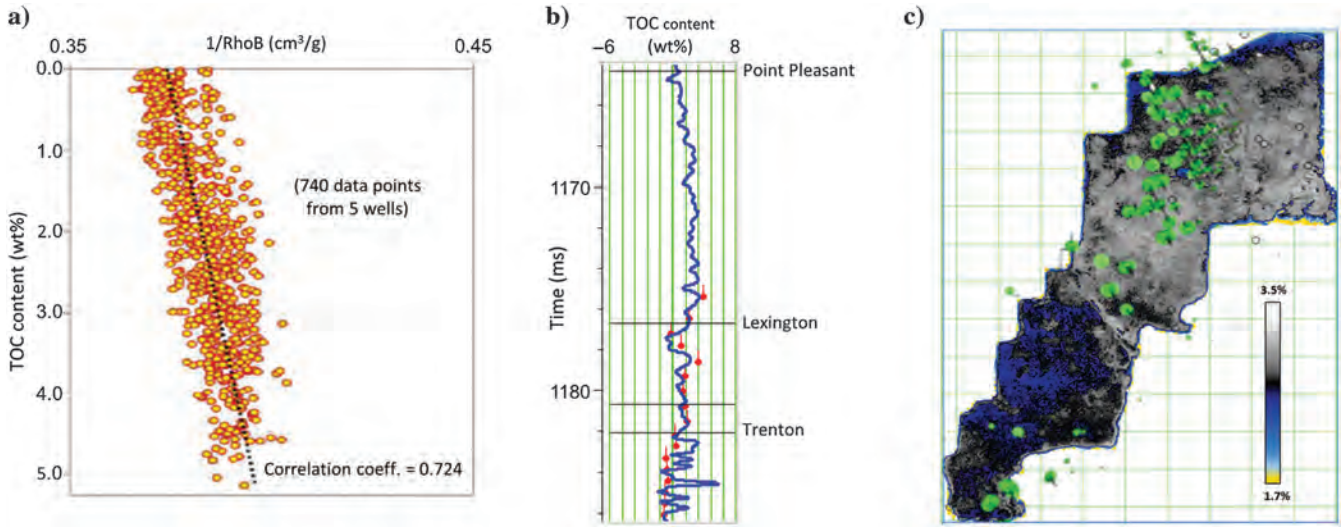

Figure 7. (a) Crossplot of bulk density from wireline logs versus TOC content from core samples in five wells from Appalachian Basin. The linear relationship between them was calibrated with core data available regionally and used to transfer density into TOC volume (adapted from Wang et al., 2016). (b) Comparison of the predicted TOC (blue) and TOC measured from the core samples for the area of study when the linear relationship (left) was used for its prediction. A reasonable match between them endorses the relationship used for the transformation. (c) Horizon slice from the predicted TOC volume more than a 10 ms window in the ZOI. Low-TOC zones are indicted by yellowish and bluish colors, whereas black and gray colors represent high-TOC zones. Notice that the northern zone exhibits the higher TOC content than of the southern zone, which is consistent with the prior information available regionally and matches the available production data (green dots).

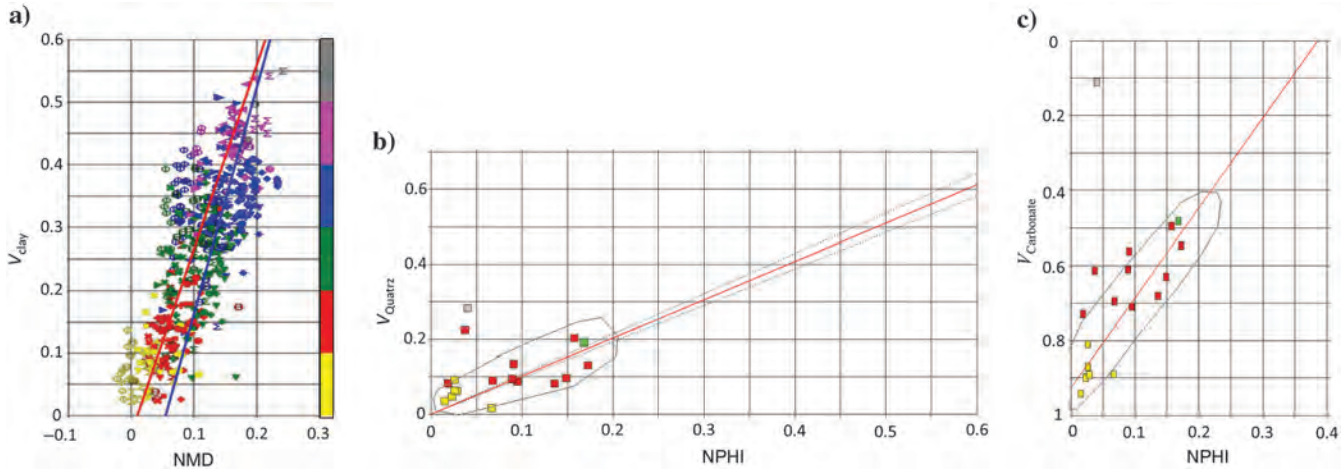

Figure 8. Petrophysical modeling reveals a strong relationship between (a) NMD and volume of clay, (b) neutron porosity and volume of quartz group, and (c) neutron porosity and volume of the carbonate group.

for some of the wells (Lear et al., 2013), and they are overlaid on the horizon slice and shown by the bigger blue circles. Thus, PIPR increases as we go from the northern to the southern part of the survey, but the mineralogical index exhibits higher values in the northern part. We explore the reasons for this discrepancy.

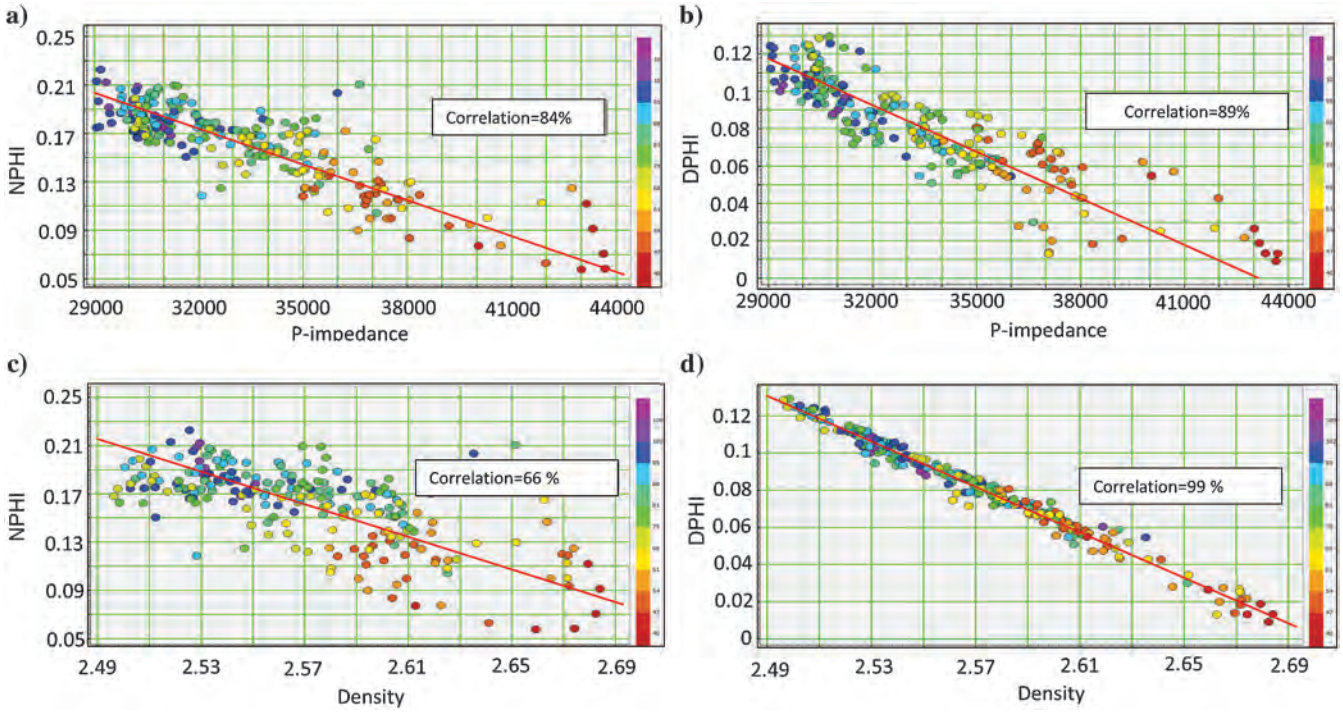

Figure 9. Crossplot of P-impedance versus (a) neutron porosity, (b) density porosity, and density versus (c) neutron-porosity and (d) density porosity, over the Point Pleasant interval. For this interval, we conclude that the P-impedance volume can be used to predict NPHI, and the density volume can be used for prediction of DPHI.

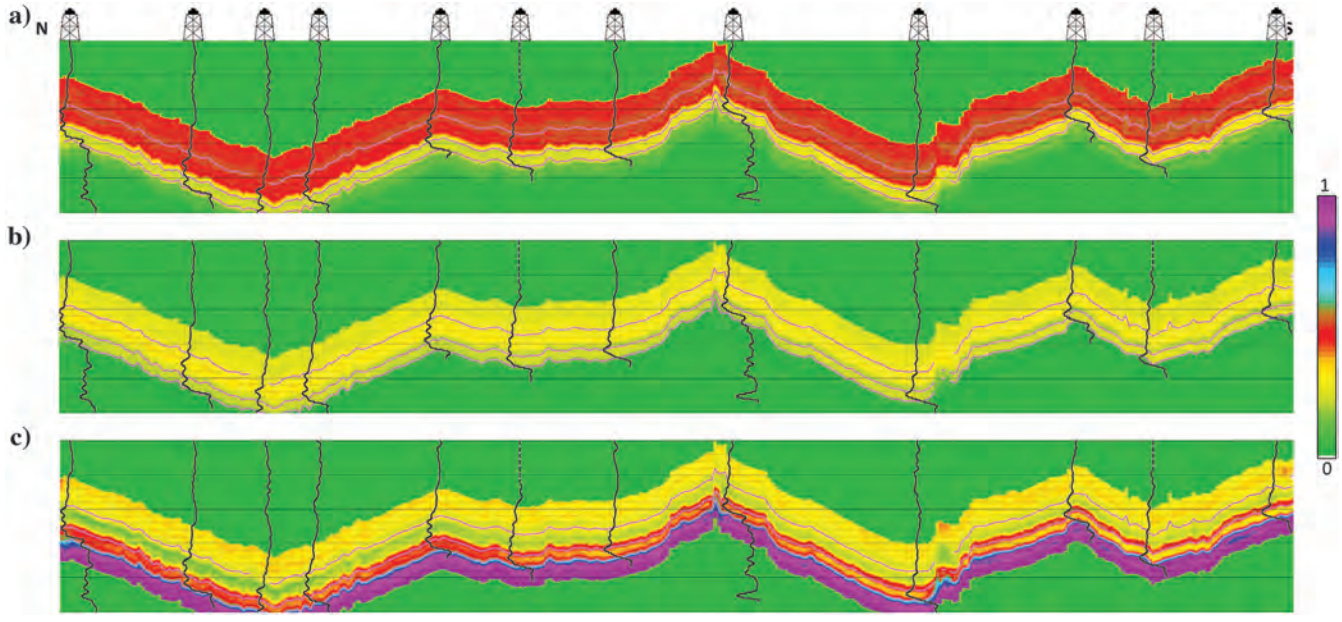

Figure 10. Arbitrary lines passing through different wells extracted from the predicted volumes of (a) clay, (b) quartz group, and (c) carbonate group. More than 40% clay content is observed in the Utica interval, and its content decreases as we go from Utica to Trenton. Quartz group content varies from 20% to 40% for the Utica and Point Pleasant intervals, whereas its content in the former interval is slightly higher than that in the latter interval. Additionally, the carbonate content decreases as we go from the Trenton to Utica intervals. Thus, Point Pleasant contains more carbonate content than the Utica interval and seems to be more brittle. This observation matches well with the available petrographic information available for the area of study and lends confidence to the prediction of different mineral contents.

Interestingly, the brittleness of a formation is enhanced by carbonates such as limestone and dolomite only up to a volume fraction of approximately 0.4. Above this value, dolomite and limestone act as fracture barriers because more energy is required to fracture shale rocks with high calcite content (Wang and Carr, 2012). This could be one of the possible reasons for having lower PIPR in the northern part than the southern within the Point Pleasant. To understand it a little more, a horizon slice from the computed carbonate content volume is extracted for the Point Pleasant interval and shown in Figure 11b. Notice that more than 40% carbonate content is present over the northern part of the display; i.e., carbonates in this zone could be acting as a fracture barrier. Therefore, mineralogical BI computation proposed by Wang and Gale (2009) may not be appropriate for the Point Pleasant interval. To overcome the shortcomings of the mineralogical BI, a fracability index (FI) has also been introduced (Jin et al., 2015). Based on the FI, high brittleness is not the only criteria for a formation undergoing good fracturing, but the requirement of less energy for creating new fractures is also important. Using the critical strain energy rate and its relationship with fracture toughness (and hence Young's modulus), the mathematical model for FI was proposed as follows:

$$\mathrm{FI} = \frac{(\mathrm{BI}_{\mathrm{mineralogy}} + E_n)}{2}, \tag{2}$$

where E_n is the inverse of normalized Young's modulus. Therefore, a formation with a higher value of FI is considered as a better fracturing target, whereas that with lower fracability is treated as a bad target.

As both the parameters required for FI estimation have already been computed, we derive that next. A horizon slice from this volume over the Point Pleasant interval is shown in Figure 11c. Notice, the southern part of Point Pleasant interval shows higher values of FI and matches reasonably well with PIPR data, which lends confidence to the whole analysis.

We next turn to making use of mechanical properties of a rock as determined by the Poisson's ratio and Young's modulus, for determination of brittleness of the zones of our interest. Different methods have been proposed for brittleness determination (Mao, 2016), but there is no one universal method that is applicable for all shale formations. We go back to one of the earlier methods proposed by Grieser and Bray (2007) for brittleness determination within the Barnett shale, using BI, which is a function of Poisson's ratio and Young's modulus, and is defined as follows:

$$\mathrm{BI}_{\mathrm{avg}} = \frac{E_B + \sigma_B}{2},$$
$$\text{where } E_B = \frac{E - E_{\min}}{E_{\max} - E_{\min}}, \quad \text{and} \quad \sigma_B = \frac{\sigma - \sigma_{\max}}{\sigma_{\min} - \sigma_{\max}}. \tag{3}$$

Following the above workflow, $\mathrm{BI}_{\mathrm{avg}}$ was computed using inverted P-, S-impedances, and the predicted density. A horizon slice from this volume over the Point Pleasant interval is shown in Figure 12a. Again, it can be noticed here that southern part of the Point Pleasant interval exhibits higher values of $\mathrm{BI}_{\mathrm{avg}}$ and seems to follow the trend noticed on the similar horizon slice of FI. This observation begs the question as to which zone should be considered for further development/drilling within the study area. To target a zone, besides brittleness or fracability information, organic richness is another important factor to be considered. The organic richness was determined through TOC content, which was derived by transforming the computed density volume. The core-log petrophysical modeling provided the

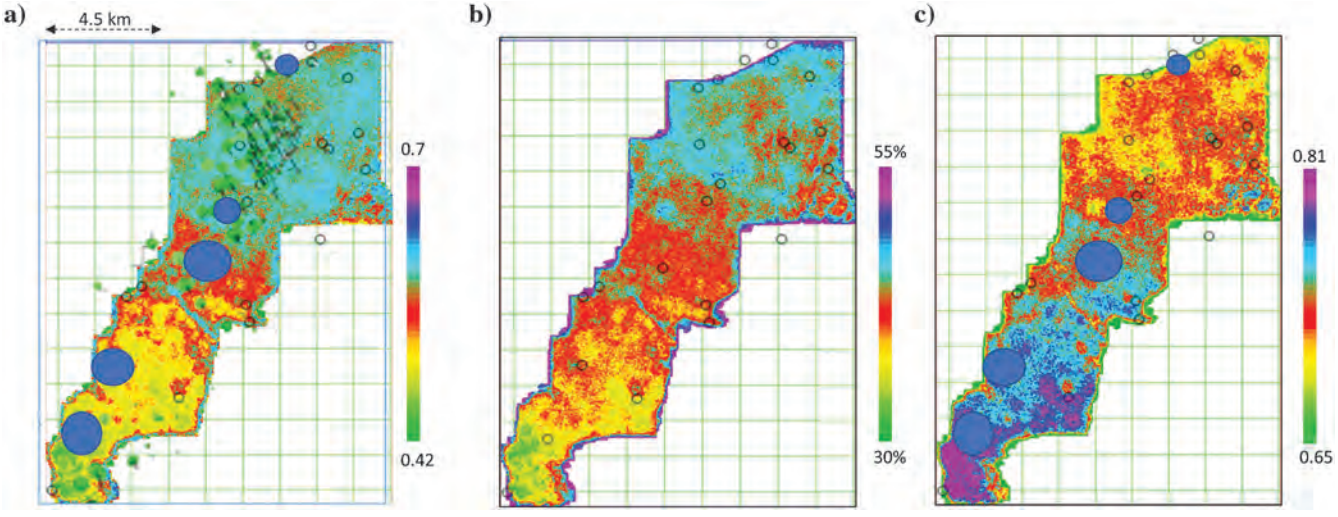

Figure 11. Horizon slices from (a) mineralogical BI. Available production data (green dots) match well with the area of higher BI; however, the available PIPR (blue dots) seems to exhibit a reverse relationship with BI, as seen by the size of the blue dots, which corresponds with the numerical values of PIPR and (b) predicted volume of carbonate over the Point-Pleasant interval. Notice, more than 40% carbonate content is seen to exist over the northern area of Point Pleasant. (c) FI, where high PIPR seems to match the high value of FI.

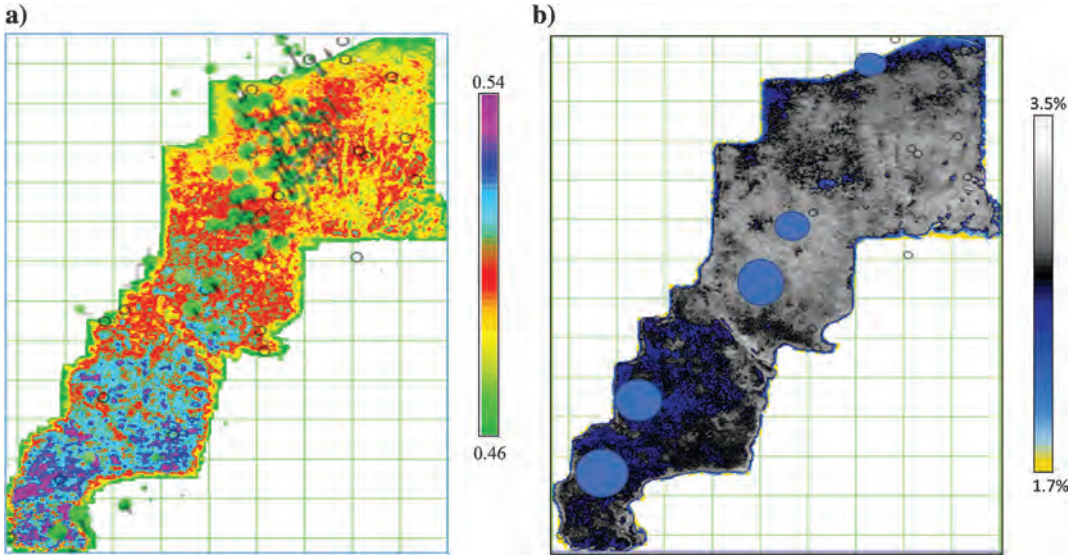

Figure 12. Horizon slices from the (a) computed BI_{avg}, (b) predicted TOC volume in the zone of interest. BI_{avg} follow a trend similar to that of *FI*. Higher values of BI_{avg} are correlating reasonably well with the higher values of PIPR. However, the threshold value of TOC used to identify the organic-rich parts reveals that the whole Point Pleasant interval can be considered a as shale play. Thus, pockets with the high FI and high BI_{avg} must be considered for further drilling.

necessary relationship for doing so. A horizon slice generated from the TOC volume over Point Pleasant interval is shown in Figure 12b. Low-TOC zones are indicted by yellow and blue colors, whereas black and gray colors represent high-TOC zones. Notice that the northern part exhibits higher TOC content than the southern part, which is consistent with the prior information available regionally. However, it is also interesting to observe that the TOC content over southern part of the Point Pleasant interval is still more than 2%, which is a threshold used for identifying a successful shale play per the organic richness. Consequently, we believe that the southern part of the Point Pleasant interval must be considered for further drilling in the area of study based on the fact that this zone contains more than 2% TOC with higher FI and BI_{avg}, which also shows the consistency with available higher PIPR.

Conclusion

In this study, an attempt has been made to characterize the Point Pleasant interval of the Utica Formation in eastern Ohio using surface seismic data, available well-log data, and other relevant data through identifying the intervals that exhibit higher TOC and higher brittleness. Knowing a strong relationship between density and TOC, a methodology was proposed to predict a reliable P-wave velocity at a sufficient number of uniformly distributed wells, so that neural network analysis was executed to determine density volume. Considering the importance of brittleness and its association with the mineralogical content of a formation, we also concluded that mineralogical BI proposed in 2015 was useful for area of study due to high carbonate content in the target formation. Regional petrophysical modeling and crosscorrelation analysis allowed us to compute mineralogical BI from surface seismic data. Although a match between mineralogical BI and production data is noticed, PIPR showed an opposite trend with mineralogical BI. FI was then used to get a somewhat better idea about favorable fracturing zones. FI showed the opposite trend to the mineralogical BI and matched well with PIPR. Thereafter, mechanical properties were considered to identify the brittle zones based on the BI_avg. A resemblance was noticed in identifying the favorable zones for drilling based on FI and BI_avg. Furthermore, TOC volume was brought into the analysis, and it was concluded that the whole Point-Pleasant interval could be treated as organically rich. Thus, zones with higher FI and BI_{avg} should be considered for further development in the area of study.

Acknowledgments

We wish to thank Arcis Seismic Solutions, TGS for encouraging this work and for the permission to present and publish it.

References

Chopra, S., R. K. Sharma, J. Keay, and K. J. Marfurt, 2012, Shale gas reservoir characterization workflows: 82nd Annual International Meeting, SEG, Expanded Abstracts, doi: 10.1190/segam2012-1344.1.

Chopra, S., R. K. Sharma, H. Nemati, and J. Keay, 2017, Seismic reservoir characterization of Utica-Point Pleasant shale with efforts at quantitative interpretation: A case study: 87th Annual International Meeting, SEG, Expanded Abstracts, 4007–4011, doi: 10.1190/segam2017-17734260.1.

Chopra, S., R. K. Sharma, H. Nemati, and J. Keay, 2018, Seismic reservoir characterization of Utica-Point Pleas-

ant shale with efforts at quantitative interpretation — Part 1: A case study: Interpretation, **6**, this issue, doi: 10.1190/int-2017-0135.1.

Grieser, B., and J. Bray, 2007, Identification of production potential in unconventional reservoirs: Presented at the SPE Production and Operations Symposium.

Hampson, D., J. S. Schuelke, and J. A. Quirein, 2001, Use of multi-attribute transforms to predict log properties from seismic data: Geophysics, **66**, 220–236, doi: 10.1190/1.1444899.

Jarvie, D. M., R. J. Hill, T. E. Ruble, and R. M. Pollastro, 2007, Unconventional shale-gas systems: The Mississippian Barnett shale of north-central Texas as one model for thermogenic shale-gas assessment: AAPG Bulletin, **91**, 475–499, doi: 10.1306/12190606068.

Jin, X., S. N. Shah, and J. C. Roegiers, 2015, An integrated petrophysics and geomechanics approach for fracability evaluation in shale reservoirs: SPE Journal, **20**, 518–526, doi: 10.2118/168589-PA.

Lear, M., D. Lee, S. Thapa, E. Westlake, A. Jayaram, H. Xu, R. Advani, and S. Willis, 2013, Equity research, exploration and production, credit Suisse, %https://research-doc.credit-suisse.com/docView?language=ENG&source=emfromsendlink&format=PDF&document_id=1020529381&extdocid=1020529381_1_eng_pdf&serialid=C91lugODraW4u9FdDgwBMrYIrRb7JKv3ytBVyGDTy6Q%3d, accessed 21 March 2017.

Leiphart, D. J., and B. S. Hart, 2001, Case history comparison of linear regression and a probabilistic neural network to predict porosity from 3-D seismic attributes in Lower Brushy Canyon channeled sandstones, southeast New Mexico: Geophysics, **66**, 1349–1358, doi: 10.1190/1.1487080.

Mao, B., 2016, Why are brittleness and fracability not equivalent in designing hydraulic fracturing in tight shale gas reservoirs: Petroleum, **2**, 1–19, doi: 10.1016/j.petlm.2016.01.001.

Patchen, D. G., and K. M. Carter, eds., 2012, A geologic play book for Utica shale Appalachian Basin Exploration, http://marcellusdrilling.com/2015/07/wvu-research-shock-finding-utica-is-as-big-as-marcellus/, accessed 27 March 2017.

Sharma, R. K., and S. Chopra, 2015, Determination of lithology and brittleness of rocks with a new attribute: The Leading Edge, **34**, 936–943, doi: 10.1190/tle34080936.1.

Verma, S., T. Zhao, K. J. Marfurt, and D. Devegowda, 2016, Estimation of total organic carbon and brittleness volume: Interpretation, **4**, no. 3, T373–T385, doi: 10.1190/int-2015-0166.1.

Wang, F. P., and J. F. Gale, 2009, Screening criteria for shale-gas system: Gulf Coast Association of Geological Societies Transactions, **59**, 779–793.

Wang, G., and T. R. Carr, 2012, Methodology of organic-rich shale lithofacies identification and prediction: A case study from Marcellus shale in the Appalachian Basin: Computers & Geosciences, **49**, 151–163, doi: 10.1016/j.cageo.2012.07.011.

Wang, G., A. Shakarmi, and J. Bruno, 2016, TOC content distribution features in Utica-Point Pleasant Formations, Appalachian Basin: Unconventional Resources Technology Conference (URTeC), 2449707, doi: 10.15530/urtec-2016-2449707.

Ritesh Kumar Sharma received a master's degree (2007) in applied geophysics from the Indian Institute of Technology, Roorkee, India, and an M.Sc. (2011) in geophysics from the University of Calgary. He works as an advanced reservoir geoscientist at Arcis Seismic Solutions, TGS, Calgary. He is involved in deterministic inversions of poststack, prestack, and multicomponent data, in addition to AVO analysis, thin-bed reflectivity inversion, and rock-physics studies. Before joining the company in 2011, he served as a geophysicist at Hindustan Zinc Limited, Udaipur, India. He won the best poster award for his presentation titled "Determination of elastic constants using extended elastic impedance," at the 2012 GeoConvention. He also received the Jules Braunstein Memorial Award for the best AAPG poster presentation titled "New attribute for determination of lithology and brittleness," at the 2013 AAPG Annual Convention & Exhibition. He received the CSEG Honorable Mention for the Best Recorder Paper award in 2013. He is an active member of SEG and CSEG.

Satinder Chopra has 30 years of experience as a geophysicist specializing in the processing, reprocessing, special processing, and interactive interpretation of seismic data. He has rich experience in processing various types of data such as vertical seismic profiling, well log data, and seismic data, as well as excellent communication skills, as evidenced by the several presentations and talks delivered and books, reports, and papers written. He has been the 2010–2011 CSEG Distinguished Lecturer, the 2011–2012 AAPG/SEG Distinguished Lecturer, and the 2014–2015 EAGE e-Distinguished Lecturer. His research interests focus on techniques that are aimed at characterization of reservoirs. He has published eight books and more than 340 papers and abstracts and likes to make presentations at any beckoning opportunity. His work and presentations have won several awards, the most notable ones being the CSEG Honorary Membership (2014) and Meritorious Service (2005) Awards, 2014 APEGA Frank Spragins Award, the 2010 AAPG George Matson Award and the 2013 AAPG Jules Braunstein Award, SEG Best Poster Awards (2007, 2014), CSEG Best Luncheon Talk award (2007), and several others. He is a member of SEG, CSEG, CSPG, EAGE, AAPG, and the

Association of Professional Engineers, Geologists, and Geophysicists of Alberta.

James Keay has more than 30 years of experience in international oil and gas exploration, development, and operations, onshore and offshore. He has extensive experience in business development and operations management in North America, Latin America, and the Middle East and has performed integrated reservoir studies in Canada, Colombia, and Kuwait. He holds a Texas Professional Geoscientist License. As chief geologist, NSA, he is responsible for providing geoscience evaluations to grow TGS's investment and sales activities.

Hossein Nemati is a geoscientist with Arcis/TGS in Calgary. He is an interpretation geoscientist and performs evaluation of resource plays and supports Arcis/TGS Multi-Client business. He has worked on a variety of play including unconventional plays in basins across North America. Before joining Arcis, he worked as geomodeler and gained experience in reservoir characterization in several field development projects in Iran. He has dual background educations in petroleum engineering and geoscience. He is a graduate of the Integrated Petroleum Geosciences (IPG) program at the University of Alberta and is currently a member of AAPG, SPE, CSEG, and CSPG.

Larry Lines received a B.S. (1971), an M.S. (1973) in geophysics from the University of Alberta, and a Ph.D. (1976) in geophysics from the University of British Columbia. His industrial career included 17 years with Amoco in Calgary and Tulsa (1976–1993). Following a career in industry, he held the NSERC/Petro-Canada chair in applied seismology at Memorial University of Newfoundland (1993–1997) and the chair in Exploration Geophysics at the University of Calgary (1997–2002). From 2002 to 2007, he served as the head of the Department of Geology and Geophysics at the University of Calgary. In professional service, he was the president of SEG in 2008–2009. Previous to that, he served SEG as geophysics editor (1977–1999), distinguished lecturer, GEOPHYSICS associate editor, translations editor, publications chairman, and as a member of *The Leading Edge* editorial board. He has served as CJEG editor twice. He and co-authors have won SEG's Best Paper in GEOPHYSICS Award twice (1988, 1995) and have twice won Honorable Mention for Best Paper (1986, 1998). Larry is an honorary member of SEG, CSEG, and the Geophysical Society of Tulsa, and he is a Fellow of Geoscientists Canada. In 2017, he received the CSEG Medal, the highest honor that CSEG bestows, in recognition of his contributions to Exploration Geophysics in Canada. Additionally, he is a member of APEGGA, CGU, EAGE, and AAPG.